Oxidation of Water by MnO_4^- mediated by Thermally Activated Ruthenium Dioxide Hydrate

Andrew Mills,* Peter Douglas and Tom Russell
Department of Chemistry, University College of Swansea, Singleton Park, Swansea SA2 8PP, UK

The kinetics of oxidation of water to oxygen by MnO_4^-, mediated by thermally activated ruthenium dioxide hydrate, has been studied. The rate of catalysis is 0.8 order with respect to the surface concentration of MnO_4^- (which in turn appears to fit a Langmuir adsorption isotherm) and proportional to the catalyst concentration, but is independent of the concentration of manganese(II) ions. The catalysed reaction appears to have an activation energy of 50 ± 1 kJ mol^{-1}. These observed kinetics are readily rationalised using an electrochemical model in which the catalyst particles act as microelectrodes providing a medium for electron transfer between the highly irreversible oxidation of water to O_2 and the highly irreversible reduction of MnO_4^- to Mn^{2+}.

There are many inorganic redox reactions of the type (1) which, although thermodynamically feasible, do not normally proceed

$$n_1Ox^2 + n_2Red^1 \longrightarrow n_1Red^2 + n_2Ox^1 \qquad (1)$$

at a discernible rate.[1,2] Many classic examples are to be found in the oxidation of water to oxygen by a suitably strong oxidising agent, Ox, *i.e.* as in equation (2). It is well recognised that

$$4Ox + 2H_2O \longrightarrow 4Red + 4H^+ + O_2 \qquad (2)$$

reaction (2) does not proceed under ambient conditions using the following common strong oxidants (Ox) despite, in each case, a high thermodynamic feasibility: IO_4^-, BrO_3^-, MnO_4^- or Ce^{IV}.[3] Lack of reaction as in equation (2) has the advantage that aqueous acidic solutions of the above oxidants are stable over long periods of time and, therefore, often convenient for carrying out oxidation reactions other than (2). Indeed, the combination of high oxidation potential and aqueous solution stability has led to the widespread use of such oxidants in aqueous redox analytical chemistry.[4]

In some situations, however, the lack of reaction when thermodynamically feasible can be an undesirable feature. For example, a great deal of solar-energy research has been directed towards the development of efficient photosystems for the cleavage of water into hydrogen and oxygen. In such a system reaction (2) must occur at some stage using an oxidising agent which has been photogenerated directly or indirectly.[5] Thus, the recognised improbability of reaction (2) occurring in homogeneous solution for most oxidants poses a major problem to the development of an overall water-splitting system.

It is possible to facilitate many of the redox reactions described by reaction (1) through the use of a redox catalyst. As a consequence a considerable amount of research has been dedicated to finding a stable, active catalyst for reaction (2). Research carried out by our group has shown that this reaction, with Ox = Ce^{IV}, is mediated by a partially dehydrated form of ruthenium dioxide hydrate (*ca.* 10% H_2O), which we have called 'thermally activated ruthenium dioxide hydrate', or $RuO_2{\cdot}yH_2O^*$ for short [$RuO_2{\cdot}yH_2O^*$ is prepared by annealing highly hydrated ruthenium dioxide hydrate (the usual form of this oxide hydrate available commercially; ≥24% H_2O) in air (or nitrogen) for 5 h at 144 °C].[6] This material is one of the first highly reliable O_2 catalysts [*i.e.* for the oxidation of water as in equation (2)] to be developed, however detailed studies of how it works have only just begun.[3] An important aspect of this work is the study of the effect model oxidants of different electrochemical reversibilities have on the kinetics of O_2 catalysis. The more electrochemically reversible a redox couple is, the faster the exchange of the electrons between its oxidised and reduced forms occurs at the electrode (redox catalyst) in question, and the most marked examples of redox catalysis are usually when a highly irreversible reaction is coupled to a highly reversible reaction.[3] The results of such work are likely to be very useful in the development of efficient photochemical systems for water cleavage.

The results of a detailed study of the kinetics of reaction (2), with Ox = Ce^{IV} as our model oxidant, were readily interpreted using an electrochemical model in which the redox catalyst particles of $RuO_2{\cdot}yH_2O^*$ were considered to act as microelectrodes mediating electron transfer between a Nernstian reduction reaction ($Ce^{IV} \longrightarrow Ce^{III}$) and an irreversible oxidation reaction ($H_2O \longrightarrow 2H^+ + \frac{1}{2}O_2$).[7] The electrochemical reduction of MnO_4^- to Mn^{2+}, unlike that of Ce^{IV} to Ce^{III}, is known to be a highly irreversible process.[8] Thus, in this paper we examine an alternative electrochemical model of oxygen catalysis through a kinetic study of reaction (2), mediated by $RuO_2{\cdot}yH_2O^*$, using the highly coloured, multi-oxidising oxidant MnO_4^- as our model. To our knowledge no detailed kinetic study of oxygen catalysis using a multioxidising oxidant has been reported previously.

Experimental

Materials.—The catalyst $RuO_2{\cdot}yH_2O^*$ was prepared from highly hydrated ruthenium dioxide hydrate obtained from Johnson Matthey.[6] All other chemicals were obtained from BDH in AnalaR form. All water used in the preparation of solutions was doubly distilled and deionised.

Methods.—The experimental system used to monitor the reduction of the oxidant MnO_4^- and concomitant evolution of O_2 as a function of time has been described previously.[9] Each stock solution of $KMnO_4$ used (6.5×10^{-3} mol dm^{-3}) was made up in 1 mol dm^{-3} $HClO_4$, unless stated otherwise. The concentration of the stock catalyst dispersion was, typically, 15 μg cm^{-3} made up in 1 mol dm^{-3} $HClO_4$.

In a typical experiment 65 cm^3 of the stock catalyst dispersion were placed in the reaction vessel and nitrogen purged for 20

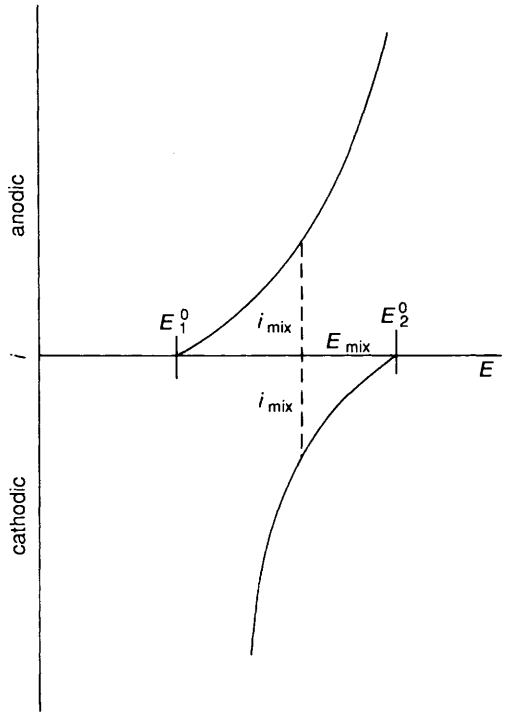

Fig. 1 Schematic illustration of the relevant current *vs.* voltage curves for the redox couples Ox^1–Red^1 and Ox^2–Red^2 with the redox catalyst as the working electrode. The electrochemical model of redox catalysis assumes that at any time t during catalysis the redox catalyst is poised at a mixture potential, $E_{mix,t}$, so that $i_{a,t} = -i_{c,t} = i_{mix,t}$. In the MnO_4^-–H_2O system it is assumed that $i_{mix,t}$ lies in the Tafel region of both current *vs.* voltage curves

min; the reaction vessel comprised a thermostatted quartz cell (30 ± 0.05 °C) with an oxygen membrane polarographic detector incorporated into its base. The kinetic run was started by injecting into the catalyst dispersion in the reaction vessel a small volume (typically 1.0 cm^3) of the oxidant stock solution. Spectrophotometric monitoring of the oxidant concentration was achieved using an optical system comprising light source, reaction vessel, monochromator, amplifier and microcomputer; the cell path length was always 3.2 cm. The absorbance *vs.* time profile was recorded, stored and subsequently analysed using an Achimedes BBC microcomputer. The concentration of dissolved O_2 in the reaction vessel was monitored as a function of time using the membrane detector. The number-average particle size in a stock dispersion of $RuO_2{\cdot}yH_2O$* was determined as 6.10 μm by dynamic light scattering (Malvern Mastersizer).

Electrochemical Model

In the many examples of redox catalysis the catalyst appears simply to provide a medium through which electron transfer from one redox couple to another can occur. This electrochemical approach to redox catalysis allows the kinetics of catalysis to be predicted from the current *vs.* voltage curves for the two contributing couples provided the two redox couples act independently of each other (the Wagner–Traud additivity principle).[1]

In this model of catalysis of the general reaction (1), at any time t during the course of catalysis the catalyst adopts a mixture potential, $E_{mix,t}$, at which the cathodic current, $i_{c,t}$, due to the reduction of Ox^2 is exactly balanced by the anodic current, $i_{a,t}$, due to the oxidation of Red^1. Although the net current is zero, the numerical magnitude of each component current is the same and is called the mixture current, $i_{mix,t}$ [equation (3)]. In our specific study of the catalysis of reaction

$$i_{mix,t} = i_{a,t} = -i_{c,t} \quad (3)$$

(2), with $Ox^2 = MnO_4^-$, by particles of $RuO_2{\cdot}yH_2O$* dispersed in solution, at any time t during catalysis the particles can be envisaged as acting as a collection of microelectrodes, each poised at $E_{mix,t}$.

The current *vs.* voltage curve for the oxidation of Red^1 to Ox^1, where $Red^1 = H_2O$ and $Ox^1 = O_2$, is, for most materials including RuO_2 macroanodes,[10] adequately described by a Tafel-type equation, *i.e.* (4) where α_1, is the transfer coefficient

$$i_a = i_{01}\exp(\alpha_1 F\eta_1/RT) \quad (4)$$

and η_1 is the overpotential. The overpotential is given by equation (5) where E_1 is the equilibrium potential for the Ox^1–Red^1 couple. The stoichiometric electrode process of any given redox couple can be written as in equation (6) where S_j

$$v_aS_a + v_bS_b + \cdots + v_jS_j + ne^- = 0 \quad (6)$$

represents the formula of species j and where the stoichiometric coefficients, v_j, are positive for oxidants and negative for reductants. In the presence of an excess of inert supporting electrolyte the corresponding Nernst equation for the equilibrium potential, E, is then (7).

$$E = E^\circ + (RT/nF)\Sigma v_j \ln(c_j) \quad (7)$$

In our work, the concomitant reduction of Ox^2 to Red^2 is the reaction $MnO_4^- \longrightarrow Mn^{2+}$ which, from previous electrochemical studies, is likely to be a highly irreversible process.[2,8] As a result, the corresponding current *vs.* voltage curve should be given by a Tafel-type expression (8). The exchange current

$$i_c = i_{02}\exp(-\alpha_2 F\eta_2/RT) \quad (8)$$

densities, i_{01} and i_{02}, are given by expressions (9) and (10)

$$\ln(i_{01}) = \ln(i_{001}) + (\theta_1 + \alpha_1 v_1/n_1)\ln[Red^1] \quad (9)$$

$$\ln(i_{01}) = \ln(i_{002}) + (\theta_2 - \alpha_2 v_2/n_2)\ln[Red^2] \quad (10)$$

where θ_1 and θ_2 are, respectively, the electrochemical reaction orders of Red^1 and Ox^2 in the anodic and cathodic processes occurring on the surface of the redox catalyst. The terms i_{001} and i_{002} are the standard exchange current densities for the couples Ox^1–Red^1 and Ox^2–Red^2, respectively.

Spiro[11] has considered this particular electrochemical model of redox catalysis, schematically illustrated in Fig. 1, and shown that the mixture current at any time t during the reaction will be given by equation (11) where r_1 and r_2 are defined in (12).

$$i_{mix,t} = i_{001}r_2\, i_{002}r_1[Red^1]\theta_1 r_2[Ox^2]\theta_2 r_1 \exp[\alpha_2 r_1 F(E_2^\circ - E_1^\circ)/RT] \quad (11)$$

$$r_1 = \alpha_1/(\alpha_1 + \alpha_2);\ r_2 = \alpha_2/(\alpha_1 + \alpha_2) \quad (12)$$

In the case of reaction (2), equation (11) reduces to (13) where

$$i_{mix,t} = K_1 i_{001}r_2{\cdot}i_{002}r_1{\cdot}[Ox^2]\theta_2 r_1 \exp[\alpha_2 r_1 F(E_2^\circ - E_1^\circ)/RT] \quad (13)$$

$K_1 = [H_2O]\theta_1 r_2$ = constant. From equation (13) it can be seen that one of the interesting features of this particular model is that the product concentrations play no role in the forward kinetics. Such kinetics are very different to those observed for reaction (2) mediated by $RuO_2{\cdot}yH_2O$* using Ce^{IV} (in 0.5 mol dm^{-3} H_2SO_4) as the oxidant. In this latter case one of the

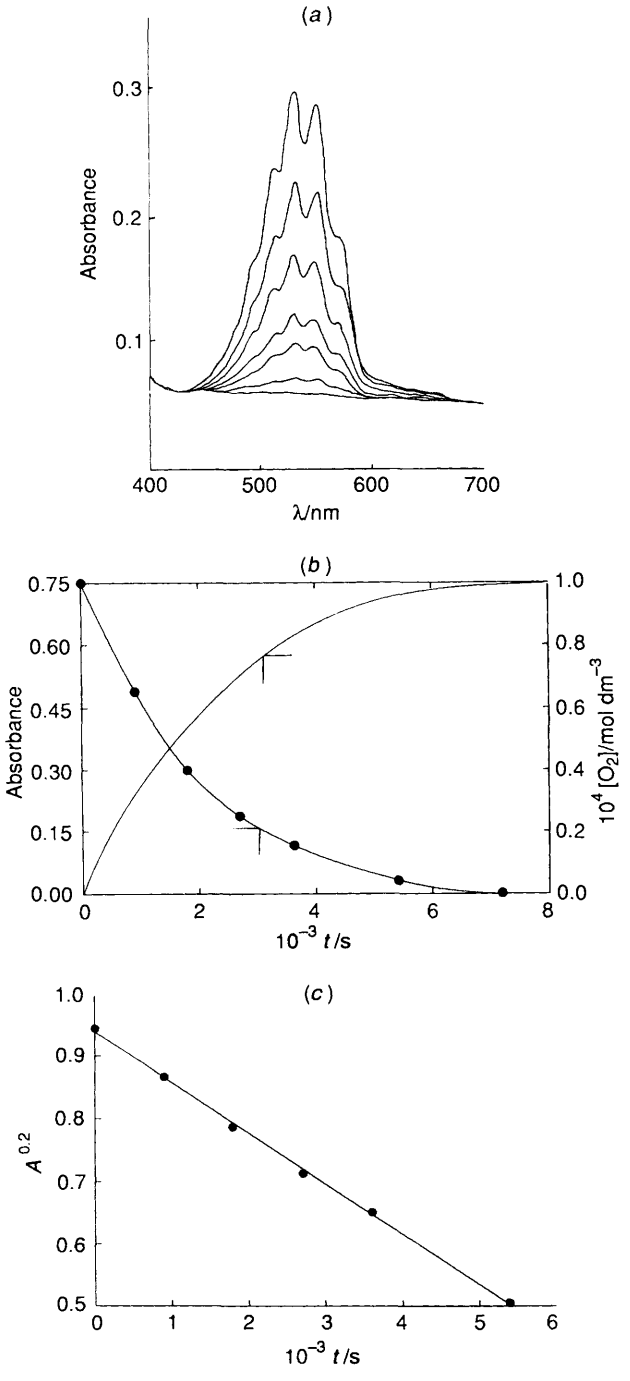

Fig. 2 Results arising from a typical kinetic run in which the reaction conditions, directly after mixing, were: $[MnO_4^-] = 10^{-4}$ mol dm^{-3}, $[RuO_2{\cdot}yH_2O^*] = 15$ μg cm^{-3}, $[HClO_4] = 1$ mol dm^{-3} and $t = 30$ °C. (*a*) Absorption spectrum of MnO_4^- *vs.* time (at 0, 15, 30, 45, 60, 90 and 120 min from top to bottom; all recorded in a 1 cm cell). (*b*) Absorbance due to MnO_4^- (at 527 nm) and concomitant $[O_2]$ evolved (overall dioxygen yield = 80%) as a function of time observed for an identical kinetic run to that in (*a*) carried out in the reaction vessel of our experimental system; path length 3.2 cm [although in this trace over 480 points were recorded, the black dots included refer to absorbances predicted from the spectral changes recorded in (*a*)]. (*c*) Plot of (Absorbance of $MnO_4^-)^{0.2}$ *vs.* time over three half-lives of the kinetic data illustrated in (*b*). A least-squares analysis revealed: number of points (n) = 480, gradient (m) = $-(8.1 \pm 0.01) \times 10^{-5}$ (absorbance units)$^{0.2}$ s^{-1}, intercept (c) = 0.938 ± 0.004 (absorbance units)$^{0.2}$ and correlation coefficient (r) = 0.999 84

products, Ce^{III}, had a marked inhibitory effect on the rate of catalysis.

Results

The MnO_4^-–Mn^{2+} couple (14) has a formal redox potential

$$MnO_4^- + 8H^+ + 5e^- \longrightarrow Mn^{2+} + 4H_2O \quad (14)$$

$E^\circ(MnO_4^-$–$Mn^{2+})$ of 1.51 V *vs.* normal hydrogen electrode (NHE) at pH 0.[2] Thus, as indicated earlier, at pH 0, MnO_4^- is thermodynamically able to oxidise water to oxygen [equation (15)] since $E^\circ(O_2$–$H_2O) = 1.23$ V *vs.* NHE. Although aqueous

$$4MnO_4^- + 12H^+ \longrightarrow 4Mn^{2+} + 6H_2O + 5O_2 \quad (15)$$

solutions (acidic, neutral or alkaline) of MnO_4^- are intrinsically unstable, their decomposition under ambient conditions is usually very slow (*i.e.* $t_{\frac{1}{2}}$ > many weeks) in the absence of bright sunlight; the latter can promote the decomposition of even the most pure MnO_4^- solution.[4]

In a typical experiment a kinetic run was carried out in a 1 cm cell, using initial concentrations (*i.e.* directly after mixing at $t = 0$) of MnO_4^- and $RuO_2{\cdot}yH_2O^*$ of 10^{-4} mol dm^{-3} and 15 μg cm^{-3}, respectively, and the resulting changes in the visible absorption spectrum of MnO_4^- as a function of time are illustrated in Fig. 2(*a*). For an identical kinetic run carried out in the reaction vessel of our experimental system, Fig. 2(*b*) illustrates the observed change of absorbance due to MnO_4^- monitored at 527 nm [$\varepsilon(MnO_4^-) = 2343$ dm^3 mol^{-1} cm^{-1}] and dissolved oxygen concentration (where 100% O_2 yield = $[O_2] = 1.25 \times 10^{-4}$ mol dm^{-3}; in this experiment O_2 yield = 80%) as a function of time. Unless stated otherwise, in this and all subsequent kinetic runs the kinetics of dioxygen generation matched those for MnO_4^- reduction, with typical overall O_2 yields of 75–80%. Repeat injections of MnO_4^- into the same catalyst dispersion gave the same yields, *i.e.* 75–80%. We believe that the other *ca.* 20% of oxidising equivalents is also used to oxidise water to O_2 *via* reaction (15), but that 100% yields of O_2 are not observed due to the slow nature of the kinetics which allows time for some partitioning of the O_2 between the aqueous phase (where the O_2 is detected) and the small head space present in the system.

It was further observed that *the kinetics of* MnO_4^- *reduction was unaltered by the initial concentration of* Mn^{2+} *present even with manganese*(II) *concentrations up to ten times that of the initial* MnO_4^-. Unless stated otherwise, in this and all other kinetic runs described in this paper the kinetics of MnO_4^- reduction were fitted excellently over three half-lives (correlation coefficient r typically > 0.9990) by assuming that the rate of reaction depends upon $[MnO_4^-]^{0.8}$ (the uncertainty in the order of the kinetics of MnO_4^- reduction with respect to $[MnO_4^-]$ is *ca.* 0.05); this is illustrated in Fig. 2(*c*) *via* a plot of $[MnO_4^-]^{0.2}$ *vs.* t using the data shown in Fig. 2(*b*). The gradient (m) of the straight line in Fig. 2(*c*) is a measure of the rate constant for the catalysed reaction which we shall refer to as $k_{0.8}$, where $k_{0.8} = -m$ in (absorbance units)$^{0.2}$ s^{-1}.

The evolution of O_2 *via* reaction (15) mediated by $RuO_2{\cdot}yH_2O^*$ was confirmed as being near stoichiometric from the membrane detector data [see Fig. 2(*b*) for example]. The concomitant generation of a stoichiometric quantity of Mn^{2+} was confirmed by filtering off the redox catalyst at the end of the reaction, oxidising the Mn^{2+} to MnO_4^- in the filtrate using a two-fold excess of solid sodium bismuthate, filtering off the excess of sodium bismuthate and recording the absorbance spectrum of the final filtrate; in all cases the latter was identical to that of the initial MnO_4^- solution.

Using all other experimental conditions the same as before, the initial rate of reaction (15) mediated by $RuO_2{\cdot}yH_2O^*$ at 30 °C was studied as a function of $[MnO_4^-]$ over the range 0–1.7×10^{-3} mol dm^{-3}. Fig. 3 illustrates a plot of initial rate R_i *vs.* $[MnO_4^-]$. As suggested by these results it was also noted that throughout the course of reaction at low $[MnO_4^-]$ (*i.e.* $\leqslant 10^{-4}$ mol dm^{-3}) the order in $[MnO_4^-]$ was 0.8, whereas at $[MnO_4^-]$ significantly greater than 10^{-3} mol dm^{-3} the rate of

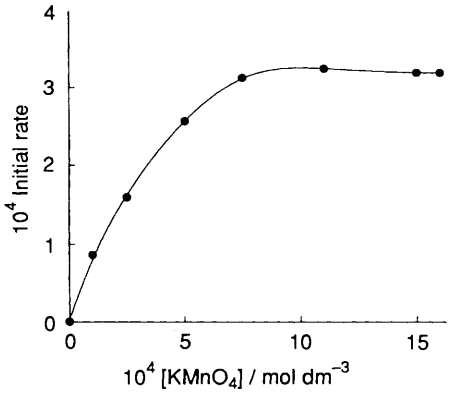

Fig. 3 Initial rate of reduction of MnO_4^- (MnO_4^- absorbance units at 470 nm per s) *vs.* $[MnO_4^-]$, with $[RuO_2{\cdot}yH_2O^*] = 15$ μg cm^{-3}, $[HClO_4] = 1$ mol dm^{-3} and 30 °C

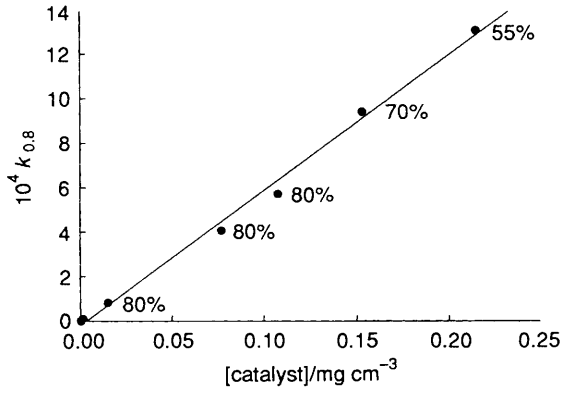

Fig. 4 Plot of $k_{0.8}$ [in (MnO_4^- absorbance units at 527 nm)$^{0.2}$ s^{-1}] *vs.* $[RuO_2{\cdot}yH_2O^*]$; reaction conditions as for Fig. 3, with $[MnO_4^-] = 10^{-4}$ mol dm^{-3}. The results of a least-squares analysis are as follows: $n = 7$, $m = (6.1 \pm 0.2) \times 10^{-3}$ (MnO_4^- absorbance units at 527 nm)$^{0.2}$ s^{-1} per mg cm^{-3}, $c = -(0.21 \pm 0.22) \times 10^{-4}$ (MnO_4^- absorbance units at 527 nm)$^{0.2}$ s^{-1} and $r = 0.9974$. % refers to the observed yields of O_2

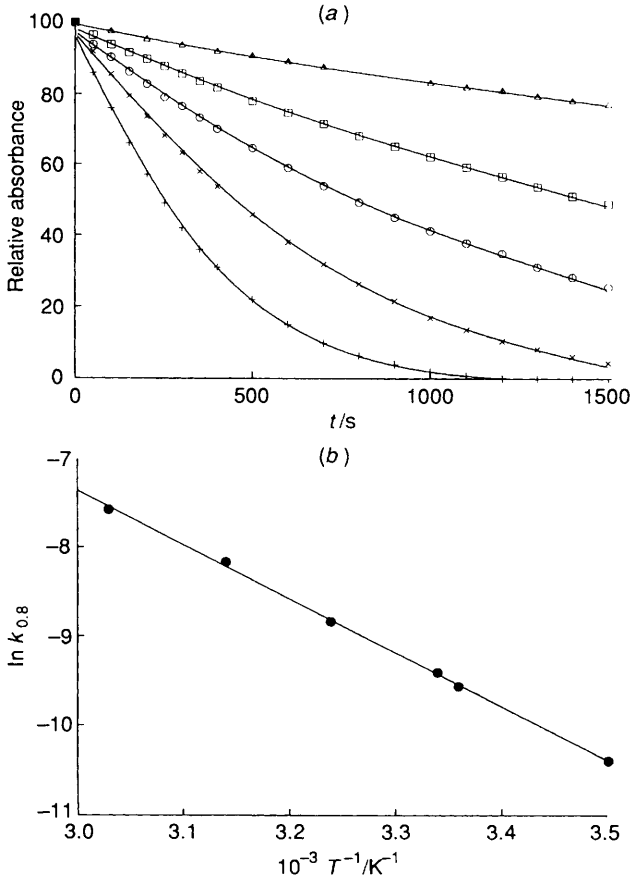

Fig. 5 Kinetic study of reaction (15) as a function of temperature; all other conditions as for Fig. 3. (*a*) Relative absorbance at 527 nm *vs.* time profiles for (from top to bottom) 12.5, 26, 35.5, 45.5 and 56 °C; a relative absorbance of 1 is equivalent to the actual absorbance of 0.75. (*b*) Arrhenius plot of ln ($k_{0.8}$) *vs.* $1/T$; a least-squares analysis of the data revealed the following: $n = 6$, $m = -(6.06 \pm 0.09) \times 10^3$ K, $c = 10.8 \pm 0.3$ and $r = 0.9995$

MnO_4^- reduction was independent of $[MnO_4^-]$, *i.e.* zero order.

Using all other reaction conditions as above, the kinetics of reaction (15) mediated by $RuO_2{\cdot}yH_2O^*$ was studied as a function of $[RuO_2{\cdot}yH_2O^*]$, over the wide range 0–215 μg cm^{-3}. In all cases the order in $[MnO_4^-]$ was 0.8 and Fig. 4 illustrates the apparent direct relationship between $k_{0.8}$ and $[RuO_2{\cdot}yH_2O]$.

A series of experiments were carried out in which the kinetics of reaction (15) mediated by $RuO_2{\cdot}yH_2O^*$, set at a concentration of 15 μg cm^{-3}, was studied as a function of temperature over the range 12.5–56 °C, using an initial $[MnO_4^-] = 10^{-4}$ mol dm^{-3}. Fig. 5(*a*) illustrates the resulting absorbance *vs.* time decays and Fig. 5(*b*) an Arrhenius plot in the form of ln($k_{0.8}$) *vs.* T^{-1} from which an activation energy of 50 ± 1 kJ mol^{-1} was calculated. The latter appears to be a reasonable value for an activation-controlled reaction and clearly different from the value of 15–19 kJ mol^{-1} typically associated with diffusion-controlled reactions.[12]

Although reaction (15) mediated by $RuO_2{\cdot}yH_2O^*$ proceeds at a measurable rate if carried out in a reaction medium of 1 mol dm^{-3} $HClO_4$, the rate is *ca.* six times slower in 1 mol dm^{-3} H_2SO_4. The inhibitory effect of H_2SO_4 was investigated further through a study of the kinetics of reaction (15), mediated by $RuO_2{\cdot}yH_2O^*$ (75 μg cm^{-3}), as a function of $[HSO_4^-]$. In all the runs made the kinetics of MnO_4^- reduction appeared to exhibit an order of 0.8 in $[MnO_4^-]$, unchanged by the presence of Mn^{2+} ions and with an overall high yield of O_2 (typically 75–80%). An important aspect of this work is the equilibrium

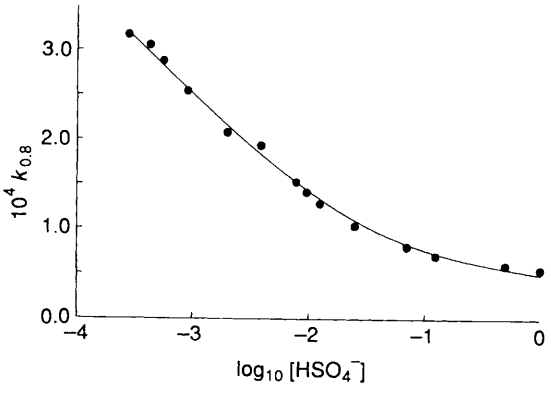

Fig. 6 Plot of $k_{0.8}$ *vs.* log$[HSO_4^-]$ using the same reaction conditions as for Fig. 3, with $[RuO_2{\cdot}yH_2O^*] = 75$ μg cm^{-3}

(16) which has a constant[13] $\approx 10^2$ mol dm^{-3}. The experimental

$$H_2SO_4 \rightleftharpoons HSO_4^- + H^+ \qquad (16)$$

conditions used were such that in each kinetic run in which $[HSO_4^-]$ (and, therefore, H_2SO_4) was varied, the 'free' $[H^+]$ was fixed at 1 mol dm^{-3}. Fig. 6 illustrates the final plot of $k_{0.8}$ *vs.* log$[HSO_4^-]$ arising from the analysis of the kinetic data obtained in this work.

Discussion

The oxidation of water by MnO_4^- *via* reaction (15) in 1 mol dm^{-3} $HClO_4$ is mediated by $RuO_2 \cdot yH_2O^*$ as evidenced by the data illustrated in Fig. 2 and the work with sodium bismuthate described earlier. The independence of the kinetics of catalysis upon $[Mn^{2+}]$ provides some supporting evidence for the applicability of the electrochemical model described earlier and summarised by equation (13). The 0.8 order with respect to $[MnO_4^-]$, observed at $[MnO_4^-] \leqslant 10^{-4}$ mol dm^{-3} [see Fig. 2(*c*)] would, according to the electrochemical model, indicate that the product $\theta_2 r_1$ is equal to 0.8 under the experimental conditions employed. Since the reaction order, θ_2, is 1 for many redox reactions, and assuming that this is also the case in our work, then it follows that r_1 must then be 0.8.

From the results of other dioxygen redox catalysis studies[7] carried out using $RuO_2 \cdot yH_2O^*$ it appears that the oxidation of water to oxygen occurs *via* the 'oxide pathway',[14] *i.e.* equations (17)–(19) where S is the surface-active site, with reaction (18) as

$$S + H_2O \longrightarrow S\text{–}OH + H^+ + e^- \quad (17)$$

$$2S\text{–}OH \longrightarrow S\text{–}O + S + H_2O \quad (18)$$

$$2S\text{–}O \longrightarrow 2S + O_2 \quad (19)$$

the rate-determining step. If it is assumed that this is also the situation for reaction (15) mediated by $RuO_2 \cdot yH_2O^*$, then the Tafel slope for water oxidation will be 30 mV per decade and, therefore, $\alpha_1 = 2$. Thus, given $r_1 = 0.8$, from equation (12) it follows that α_2 will be 0.5.

The work of Desideri[8] on the electrochemical reduction of MnO_4^- in mineral acid media using a bubbling platinum electrode confirms the highly irreversible nature of the reduction of MnO_4^- to Mn^{2+} and also indicates that α_2 may lie in the range 0.5–1. No attempt by these workers was made at interpreting these latter results in terms of an electrochemical mechanism, however one possibility can be gleaned from the work of Bockris and Reddy[15] on general multistep reactions of the type $A + ne^- \longrightarrow Z$; these workers note that if a series of quasi-electron-transfer equilibria are set up before the rate-determining step (r.d.s.) then the transfer coefficient will be given by equation (20) where γ = number of electron-transfer

$$\alpha = (\gamma/\nu) + \omega\beta \quad (20)$$

steps before the r.d.s., ν = reaction stoichiometry, β = symmetry factor and where $\omega = 1$ (if the r.d.s. is a charge-transfer step) or 0 (if the r.d.s. is a chemical reaction). Typically, $\nu = 1$ and β is taken as 0.5, thus, assuming the electrochemical model and a general multistep scheme for MnO_4^- reduction, the kinetics of MnO_4^- reduction will give a transfer coefficient $\alpha_2 = 0.5$ if the initial electron-transfer reaction involving Mn^{VII} is rate determining.

The observed variation of initial rate *vs.* $[MnO_4^-]$ illustrated in Fig. 3 appears typical of that expected if reaction (15) depends directly upon the adsorbed concentration of MnO_4^- which in turn fits a Langmuir adsorption isotherm. Assuming this adsorption isotherm and the electrochemical model, the term $[Ox^2]$ in the expression $[Ox^2]\theta_2 r_1$ in equation (13) is the concentration of adsorbed MnO_4^- per m^2 of the surface of the redox catalyst, *i.e.* as in equation (21) where $[MnO_4^-]^*$ is the

$$[MnO_4^-]_{ads} = [MnO_4^-]^* K[MnO_4^-]/(1 + K[MnO_4^-]) \quad (21)$$

concentration of MnO_4^- adsorbed per m^2 of redox catalyst when the surface has a monolayer coverage of MnO_4^- ions, K is a measure of the strength of the adsorption and $[MnO_4^-]$ is the concentration of MnO_4^- in the bulk solution. As predicted by this equation a plot of $(1/R_i)^{1.25}$ *vs* $[MnO_4^-]^{-1}$ is a good straight line, as illustrated in Fig. 7.

In the electrochemical model $i_{mix,f}$ is a current density and, therefore, will depend directly upon $-(d[MnO_4^-]/dt)$ and A_{cat}. Since the catalyst surface area will be proportional to $[RuO_2 \cdot yH_2O^*]$, the observed straight-line dependence of $k_{0.8}$ *vs.* $[RuO_2 \cdot yH_2O]$ illustrated in Fig. 4 appears to confirm the prediction made by the electrochemical model. The observed decrease in O_2 yield with increasing $[RuO_2 \cdot yH_2O^*]$ does not appear to be associated with adventitious reducible impurities associated with the $RuO_2 \cdot yH_2O^*$, since the $\%O_2$ yield remains reproducibly low for a series of repeat injections of 10^{-4} mol dm^{-3} MnO_4^- into the same catalyst dispersion. Other experiments show, under the typical experimental conditions used, that $RuO_2 \cdot yH_2O^*$; (*i*) has no strong affinity for adsorbing dissolved O_2, (*ii*) undergoes little or no corrosion and (*iii*) is charged up by the oxidant but the number of oxidising equivalents used is much lower than needed to rationalise the marked loss in O_2 yield with increasing $[RuO_2 \cdot yH_2O^*]$. At present, the most likely explanation is that as the $[RuO_2 \cdot yH_2O^*]$ is increased the fraction of O_2 generated increases on surfaces where access to the bulk solution is poor.

The variation in $k_{0.8}$ *vs.* $[HSO_4^-]$, illustrated in Fig. 6, is not simply explained and probably depends upon many factors. It could be that HSO_4^- competes with MnO_4^- for sites, however even at high $[HSO_4^-]$ an appreciable degree of catalysis continues (see Fig. 6), indicating that HSO_4^- can only bind to a limited fraction of the sites available for adsorption by MnO_4^- ions; there appears to be no obvious explanation why this should be the case. In terms of the electrochemical model the situation is further complicated by the effect of $[HSO_4^-]$ on the term $(E_2^\circ - E_1^\circ)$. Unlike the case for the Ce^{IV}–Ce^{III} couple it is not obvious why changes in $[HSO_4^-]$ should effect the equilibrium potential of the MnO_4^-–Mn^{2+} couple. However, Desideri[8] notes that the half-wave potential for the reduction of MnO_4^- to Mn^{2+} is higher in $HClO_4$ than in H_2SO_4 and at high acid concentrations (*i.e.* > 10 mol dm^{-3}) 'the permanganic ion is strongly associated with SO_4^{2-} ions to form complex ions' as evidenced by striking reversible changes in the absorption spectrum of MnO_4^- with increasing $[H_2SO_4]$; these changes are not unlike those observed for Ce^{IV} in H_2SO_4 at similar high concentrations. In addition, in the electrochemical model, if the manganese species involved in the rate-determining step is complexed by HSO_4^- then a variation in HSO_4^- will also affect the kinetics of reaction (15). It appears likely a combination of a number, if not all, of these factors is responsible for the effect of HSO_4^- on the observed variation of $k_{0.8}$ for reaction (15).

In the photochemical decomposition of MnO_4^- the origin of the oxygen is the MnO_4^- ions themselves, *via* reaction (22).[16]

$$MnO_4^- \longrightarrow MnO_2^- + O_2 \quad (22)$$

However, from the results of the work reported here there is no evidence that MnO_2 is formed and given the results of previous work on dioxygen catalytic systems using different oxidising agents[3] it appears most likely that the O_2 evolved originates from water. Further work is, however, required using isotopically labelled solvent or MnO_4^- ions to confirm this assumption.

Conclusion

The observed kinetics of the oxidation of water to oxygen by MnO_4^-, mediated by thermally activated ruthenium dioxide hydrate, is readily rationalised using an electrochemical model in which the catalyst particles act as microelectrodes providing a medium for electron transfer between the highly irreversible oxidation of water to O_2 and the highly irreversible reduction of MnO_4^- to Mn^{2+}. The rate of catalysis depends upon the surface concentration of MnO_4^- (which in turn appears to fit a Langmuir adsorption isotherm) and the catalyst concentration, but is independent of the concentration of manganese(II) ions. The results of the kinetic study indicate that the initial electron-

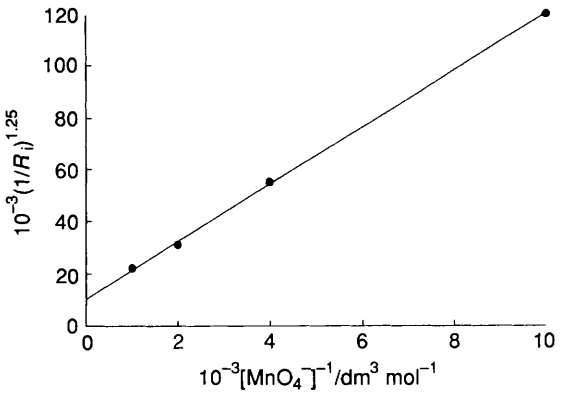

Fig. 7 Plot of the data illustrated in Fig. 3 in the form of $(1/R_i)^{1.25}$ *vs.* $[MnO_4^-]^{-1}$. The term $[MnO_4^-]$ is the total initial concentration of MnO_4^- in the bulk solution and was found to be largely unchanged after the process of adsorption of the MnO_4^- ions onto the redox catalyst. A least-squares analysis of the data revealed the following: $n = 4$, $m = 11.0 \pm 0.2$, $c = (10.4 \pm 0.9) \times 10^3$ (MnO_4^- absorbance units at 527 nm)$^{-1.25}$ $s^{1.25}$ and $r = 0.9997$

transfer reaction involving Mn^{VII} is rate determining for the reduction of the Mn^{VII}, assuming that the oxidation of water to oxygen occurs *via* the 'oxide pathway'[14] with the first disproportionation step the slowest of the steps in the oxidation of water.

Acknowledgements

We thank the University of Wales for a post-graduate studentship (for T. R.).

References

1 M. Spiro, *Chem. Soc. Rev.*, 1986, **15**, 141.
2 M. Spiro and A. B. Ravnö, *J. Chem. Soc.*, 1965, 78.
3 A. Mills, *Chem. Soc. Rev.*, 1989, **18**, 285 and refs. therein.
4 *Vogel's Quantitative Inorganic Analysis*, revised by J. Bassett, R. C. Denney, G. H. Jeffery and J. Mendham, 4th edn., Longmans, London, 1981, pp. 359 and 765.
5 *Energy Resources through Photochemistry and Catalysis*, ed. M. Grätzel, Academic Press, New York, 1983.
6 A. Mills, S. Giddings, I. Patel and C. Lawrence, *J. Chem. Soc., Faraday Trans. 1*, 1987, 2331.
7 A. Mills and N. McMurray, *J. Chem. Soc., Faraday Trans. 1*, 1989, 2055.
8 P. G. Desideri, *J. Electroanal. Chem.*, 1963, **6**, 344.
9 A. Mills and T. Russell, *J. Chem. Soc., Faraday Trans.*, 1991, 1245.
10 S. Trasatti and G. Lodi, *Electrodes of Conductive Metallic Oxides*, ed. S. Trasatti, Elsevier, Amsterdam, 1980, vol. B, ch. 10.
11 M. Spiro, *J. Chem. Soc., Faraday Trans. 1*, 1979, 1507.
12 F. Wilkinson, *Chemical Kinetics and Reaction Mechanisms*, Wiley, New York, 1981, p. 239.
13 D. F. Shriver, P. W. Atkins and C. H. Langford, *Inorganic Chemistry*, Oxford University Press, Oxford, 1990, p. 150.
14 J. O'M. Bockris, *J. Chem. Phys.*, 1956, **24**, 817.
15 J. O'M. Bockris and A. K. Reddy, *Modern Electrochemistry*, Macdonald, London, 1970, vol. 2, p. 1002.
16 G. Zimmerman, *J. Chem. Phys.*, 1955, **23**, 825.

Received 19*th July* 1991; *Paper* 1/03657B